



Finite Element Analysis of Gas Leakage Diffusion and Dynamic Response of Explosion Structure in Underground Pipe Gallery Under Different Ventilation Modes

Quanguo Han^a, Jun Dong^{b*}, Guohua Li

Beijing Higher Institution Engineering Research Center of Structural Engineering and New Materials, Beijing University of Civil Engineering and Architecture, Beijing, 100044, China;

Email: 250991147@qq.com^a; jdongcg@bucea.edu.cn^b

Abstract. With the acceleration of urbanization and the expansion of city scale, the number of super-large and megacities has increased, which has led to a new round of upsurge in the construction of underground comprehensive pipe gallery projects. In this context, the safety of gas tanks has become the focus of the design, monitoring and maintenance of pipeline corridors. This article establishes a single-chamber model of a gas tank according to the specifications, obtains the diffusion range of the explosive gas cloud through ANSYS/FLUENT, and then uses ANSYS/LS-DYNA to establish the explosion source to analyze the dynamic response of the underground pipe gallery structure. It combines new simulation ideas of diffusion and explosion to study different ventilation. The displacement force response and stress distribution of the gas tank structure under the model are used to make up for the limitations of experimental research methods such as safety risks and difficulties in reproducing working conditions. The calculation results show that the corner stress of the gas tank is the largest. Increasing the ventilation frequency of the gas tank can significantly reduce structural damage, especially for structures located in the upwind area.

Keywords: Underground utility tunnels; gas tank; gas leakage diffusion; gas explosion; dynamic response; Upwind and downwind areas.

1 Introduction

With the rapid expansion of cities in recent years, the state stipulates that gas pipelines should be separated into separate cabins and corridors with other municipal pipelines to facilitate centralized monitoring and maintenance. Among them, the safety of gas tanks has become a key issue in the design, monitoring and maintenance of pipe corridors.

When studying the problem of gas leakage and diffusion, Zhou Le et al.^[1] studied the impact of changing ventilation volume on the change of methane mass concentration in the pipe gallery under different leakage aperture conditions, and found that when

the ventilation volume was fixed, as the leakage aperture increased, However, it does not necessarily lead to the expansion of the dangerous area. The proportional relationship between ventilation volume and methane leakage should be controlled, and the volume fraction of methane should be controlled beyond the explosion limit of 5% to 15%. Chen Kun et al.^[2] studied the diffusion characteristics of methane concentration in different leak outlet directions, the concentration distribution characteristics of methane in the gallery at different leak outlet locations, the changes in gas concentration over time at different detector positions, and the different pipeline pressures and leak apertures. Effect on gas diffusion. Sun Hua, Qian Xiling, Deng Xiaojiao and others^[3-5] studied the impact of gas tank operating pipeline pressure on gas leakage diffusion and found that as the pipeline pressure increases, the detector alarm time will shorten; when the natural gas leakage pressure is the same, There is a positive correlation between gas diffusion distance and time, and there is little difference in response time to different alarm concentrations at the same location.

To study the dynamic response of structures under the action of gas explosion, Kindrack et al.^[6] experimental study showed that due to the heat exchange between thermal combustion products and cold container walls, the maximum pressure value of setting an ignition source in the central position is higher than that in other positions. Li Zhipeng et al.^[7] used the Luodai Ancient Town tunnel lining structure as the engineering background and studied the damage characteristics of gas-air premixed combustible gas as the explosion source through numerical simulation. The study found that the explosion results simulated using premixed combustible gas are more consistent with the actual situation than the simulation method using equivalent TNT equivalents. Salzano et al.^[8] conducted explosion tests on hydrogen methane air premixed gas to investigate the effects of combustible gas component concentration and initial pressure on combustion rate, peak overpressure, and overpressure rise rate.

The existing literature mostly studies the unilateral problem of leakage or explosion, and there are few studies on both problems at the same time. This paper uses ANSYS/FLUENT to obtain the diffusion range of explosive gas clouds and then uses ANSYS/LS-DYNA to establish the explosion source to analyze the dynamic response of the underground pipe gallery structure. It combines new simulation ideas of gas diffusion and explosion to study the displacement force response of the gas cabin structure under different ventilation modes. and stress distribution to make up for the limitations of experimental research methods such as safety risks and difficulties in reproducing working conditions.

2 Finite Element Model Establishment

2.1 Establishment of Gas Leakage Diffusion Calculation Model

Physical Model

According to the "Technical Specifications for Urban Comprehensive Pipe Gallery Engineering", this article stipulates that fire protection zones should be established every 200m in the gas tank, and a single fire protection zone in the gas tank is selected as the research object, with a cross-sectional size of 2.2m×3.4m. The ventilation opening and

exhaust opening are set to $1\text{m}\times 1\text{m}$, 1m away from the fire door at the end of the gas tank. According to national standards^[9], the distance between the methane sensor and the top of the gas chamber should not exceed 0.3m , and a methane detector should be installed every 15m . The design is to set the methane detector 0.2m from the top of the gas tank, and set the 20mm leak hole in the middle of the gas pipeline span with the operating pressure of the gas tank 1.6MPa at the middle position of the two methane detectors. The physical model is shown in Figure 1.

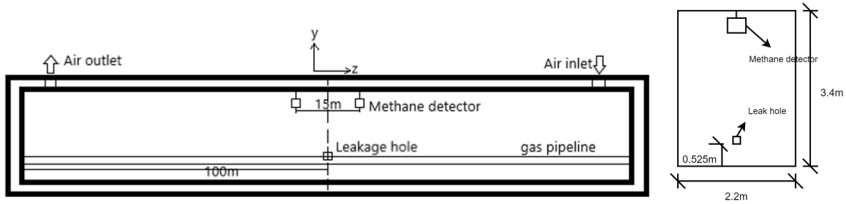


Fig. 1. Gas tank diagram

Simulation Settings

Grid setting: Create different parts of the geometric model through ICEM, divide the fluid domain into blocks, and use Hyperbolic to define hyperbolic node distribution to refine the grid near the leak hole. After passing the Jacobian ratio mesh quality judgment and angle judgment, a mesh file with a mesh number of 126,800 is output to Fluent.

Model settings: When studying the gas leakage diffusion model under different ventilation conditions, the diffusion and concentration changes of gas continue to occur over time. ANSYS/Fluent sets up a transient solution to capture these time-related changes. Select the standard $k - \epsilon$ turbulence model, activation energy equation Energy, and component transport model.

Material Settings: Set the mix material to Air and Methane.

Initial conditions: standard atmospheric pressure, gravity acceleration -9.8m/s^2 , ambient temperature 288.16K . The fluid region is locally initialized with the methane concentration set to 0.

Inlet boundary: The air inlet of the gas tank is set as the velocity outlet. According to the size of the physical model in this article, the closed condition of 0 times/h, the normal ventilation condition of 6 times/h, and the accident ventilation condition of 12 times/h in the corresponding specifications are converted into ventilation. Speed 0m/s , 2.5m/s , 5.0m/s . The leakage hole uses a mass flow inlet. According to the calculation formula in the risk-based oil and gas pipeline safety hazard classification guidelines (GB/T 34346-2017)^[10], the methane mass flow rate in this article is 0.33825kg/s .

Exit boundary: The exhaust outlet of the gas tank is set as the velocity outlet, the size is the same as the air inlet, and the direction is set in the opposite direction.

Other settings: The gas bulkhead is set to the standard wall function to handle near-wall region turbulence.

Solution settings: Use the PISO algorithm proposed by Issa to solve the pressure-velocity coupling method of transient flow. The FLUENT model of gas leakage diffusion is shown in Figure 2.

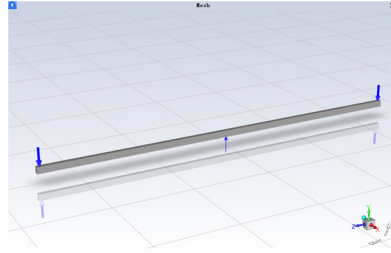


Fig. 2. FLUENT Model of Gas Leakage and Diffusion

2.2 Establishment of Gas Explosion Calculation Model

Finite Element Model.

The gas explosion calculation model intercepts the 15m fire protection zone and uses LS-DYNA modeling, in which the gas bulkhead is 0.5m thick. The model mainly studies the interaction between the gas tank, air and gas, and uses the general unit SOLID164. The Euler grid is used to simulate gas and air, while the gas tank structure uses the Lagrange algorithm. The multi-material ALE algorithm is selected to calculate the fluid-solid coupling, and the fluid-solid coupling interface is defined through the keyword *CONSTRAINED_LAGRANGE_IN_SOLID to ensure fluid mechanics and structural dynamics. Interactions between the sciences are properly simulated.

Simulation Settings.

Explosion source setting: The flammable gas method is used to simulate the explosive vapor cloud of methane-air mixture. The mixed gas explosion parameters are obtained through the Rayleigh (Eq.1) and Hugoniot (Eq.2) equations of detonation waves combined with the heat capacity method (Eq.3) and based on the chemical reaction equations of methane and air under different ventilation conditions (Tab.1).

$$p - p_0 = \frac{v_D^2}{V_0^2} (V_0 - V) \quad (1)$$

$$e - e_0 = \frac{1}{2} (p + p_0) (V_0 - V) + Q_V \quad (2)$$

$$Q_V = \sum n_i \bar{C}_{Vi} t + L \quad (3)$$

Table 1. Explosive calculation parameters for gas mixtures

Working conditions	ρ_0 (kg/cm ³)	γ	P_J (MPa)	Q_V (kJ/kg)	E_0 (kJ/m ³)
Closed	1.237	1.288	1.823	2559.34	3165.52
Normal Ventilation	1.241	1.297	1.710	2322.03	2882.53
Accident Ventilation	1.247	1.308	1.553	2018.95	2518.06

In order to facilitate the modeling analysis of LS-DYNA, Section 3.1.2 of this article first performs a preliminary fitting of the gas leakage diffusion explosion source.

However, the upper and lower limit concentration isosurfaces of methane explosion after fitting are still complex surfaces, and continue to be compiled using Python. Program to simplify loess fitting explosion sources to cylinders. The air, gas and gas compartment PART in the dynamic response damage model of the gas explosion structure under normal ventilation conditions are shown in Figure 3.

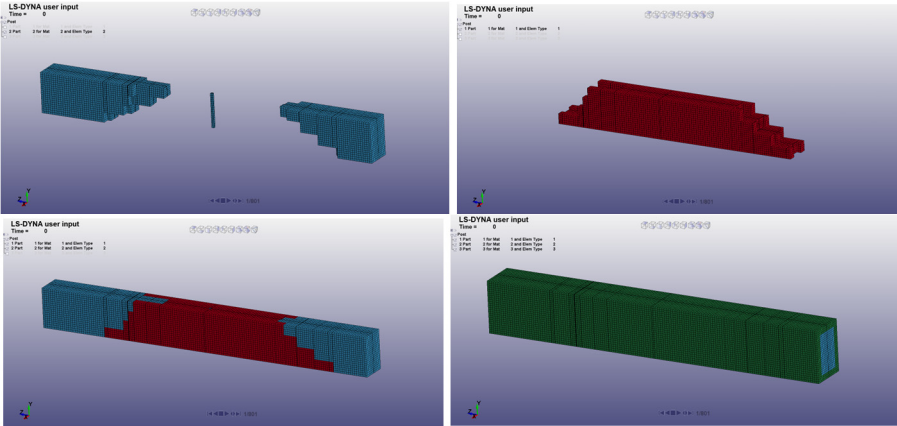


Fig. 3. Finite element model of gas tank

Material model settings: Select `*MAT_NULL` for both gas and air material models, and define them through the linear polynomial state equation `*EOS_LINEAR_POLYNOMIAL`. The material used in the gas tank in this article is reinforced concrete. Specifically, C45 grade concrete and HRB400 grade steel bars are used. The H-J-C concrete constitutive model proposed by Holmquist is used. The keyword used is `*MAT_JOHNSON_HOLMQUIST_CONCRETE`.

Boundary condition settings: fixed constraints are set at the bottom of the gas tank model, and non-reflective boundary conditions are set at the end of the gas tank to simulate the natural attenuation of the shock wave.

Keyword settings: Modify the K file keywords and add the keyword `*INITIAL_DETONATION` for the leakage hole cross-section explosion point.

Measuring Point Settings.

This article selects four longitudinal measuring points of 3m, 6m, 9m, and 12m along the longitudinal upwind and downwind areas of the mid-span leakage hole of the gas tank for comparative analysis (Figure 4). When studying displacement, select the measuring point 1 position that is greatly affected in the X direction, and the measuring point 2 position that is greatly affected in the Y direction. When studying stress distribution, select the stress The distribution affects the location of the corner areas where the roof, side walls and gas tank bulkheads meet easily.

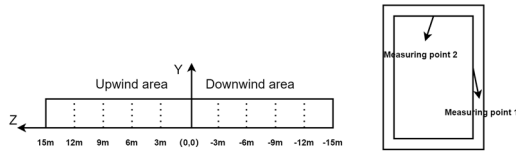


Fig. 4. Layout diagram of measurement points on the cross-section of the gas cabin

3 Simulation Result Analysis

3.1 Analysis of Numerical Simulation Calculation Results of Gas Leakage and Diffusion

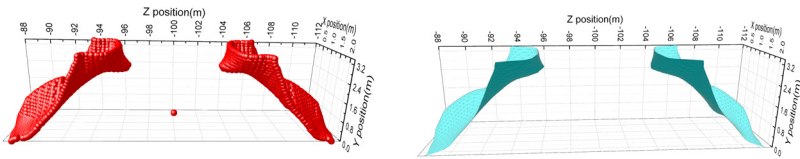


Fig. 5. Iso-surface and Loess fitting surface diagram of methane explosion lower limit concentration in a CFD model

According to the standard^[11], the alarm threshold of methane detectors in gas tanks should not be greater than 20% of the lower explosion limit of methane, that is, the alarm threshold when the volume fraction of methane is 1%.

In order to facilitate the establishment of the LS-DYNA calculation model that focuses on gas explosion-related research in this article, the explosion source in the model is first fitted to the flammable concentration cloud with a concentration of 5% to 15% in the methane explosion interval. When fitting the methane concentration range where explosions can occur, this paper uses the CFD isosurface of the methane explosion upper limit concentration of 15% and the lower limit concentration of 5% through Loess nonlinearity. Parametric regression statistical method is used to fit a low-order polynomial model near each point in the methane concentration partition. Figure 5 shows the isosurface of the methane explosion lower limit concentration in the CFD model and the fitted Loess fitting surface when gas leakage reaches the alarm threshold under closed conditions. The same fitting method is also applied to the working condition analysis of normal ventilation and accident ventilation conditions.

When the gas tank in the pipeline gallery leaks and triggers the monitoring point alarm, the concentration area above the upper limit of the gas explosion concentration (methane volume concentration is 15%) forms a columnar area that spreads upward from the leakage port to the top of the pipeline gallery. Under closed conditions, this area is fitted to a rectangular column with dimensions of $0.18\text{m} \times 0.18\text{m} \times 2.875\text{m}$; under normal ventilation conditions, it is fitted to a rectangular column of $0.1\text{m} \times 0.1\text{m} \times 2.875\text{m}$; Under accident ventilation conditions, the fitting is a rectangular columnar body of $0.08\text{m} \times 0.08\text{m} \times 2.875\text{m}$.

Table 2. The total volume and weighted volume fraction average of explosive gas equivalents

Working conditions	Total volume of isovolume (m ³)	Weighted volume fraction average (%)
Closed	113.25	8.80%
Normal Ventilation	102.26	8.06%
Accident Ventilation	71.58	7.01%

The statistics of the total volume and weighted volume fraction of the three-dimensional explosive gas equivalents in the methane range of 5% to 15% are shown in Table 2. It can be seen that as the number of ventilations increases, the leaked gas carried by the ventilation airflow flows in the downwind direction and accumulates, making the methane detector in the downwind direction reach the alarm threshold faster. The corresponding total volume and weighted volume fraction average of the corresponding explosive gas equivalents significantly reduce.

3.2 Dynamic Response of Gas Tank Structure Under Gas Explosion

Displacement Response.

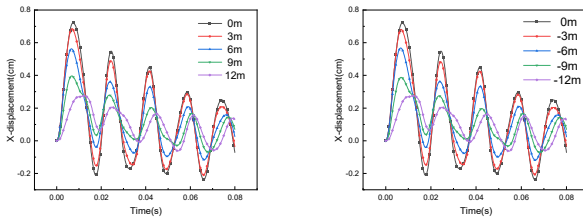


Fig. 6. Displacement changes in the X direction at measuring point 1 in the upwind and downwind areas

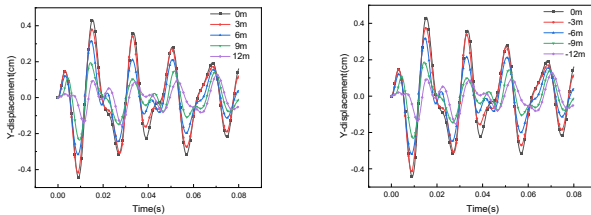


Fig. 7. Displacement changes in the Y direction at measuring point 2 in the upwind and downwind areas

Under closed conditions, it can be seen from Figure 6 and Figure 7 that the shock wave generated by the rapid increase in pressure at the moment when the gas block explodes produces an impact thrust on the wall of the gas cabin, causing the wall measuring points to be displaced, and the initial peak value of the displacement reflects The

impact intensity during the initial stage of the explosion. The shock wave first propagates along the shortest path, which is the X direction, and the peak appears first. Then, under the superposition of the initial shock wave and the reflected wave, the Y direction displacement reaches the peak at the second wave peak. Later, due to the interaction between the shock wave and the internal structure of the pipe gallery, etc. Under the influence, the energy gradually attenuates, and the displacement amplitude gradually decreases and becomes stable. The displacement change curve of structural measuring points caused by gas explosion under normal ventilation and accident ventilation conditions is the same as that under closed conditions. The stress distribution and stress time history curve of structural measuring points caused by gas explosion under normal ventilation and accident ventilation conditions are the same as those under closed conditions.

Stress Distribution in the Gas Tank.

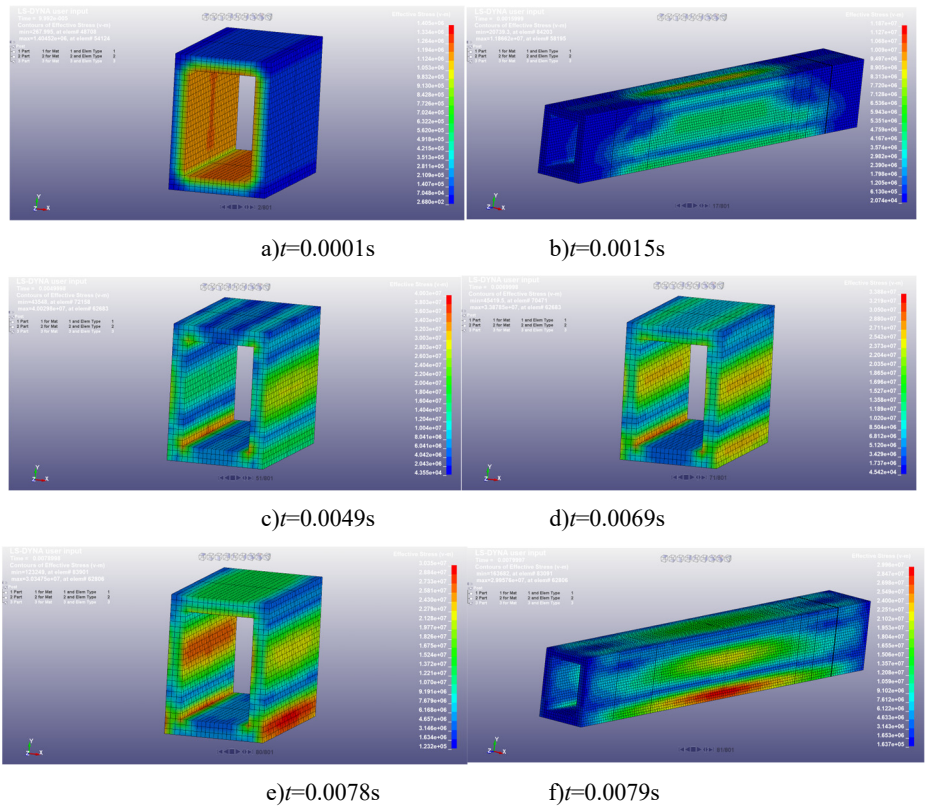


Fig. 8. Von-mises-stress cloud diagram of gas tank under accident ventilation conditions

(Note: a), c), e), f) intercepted the 6-meter-long pipe gallery section at the center of the explosive gas block)

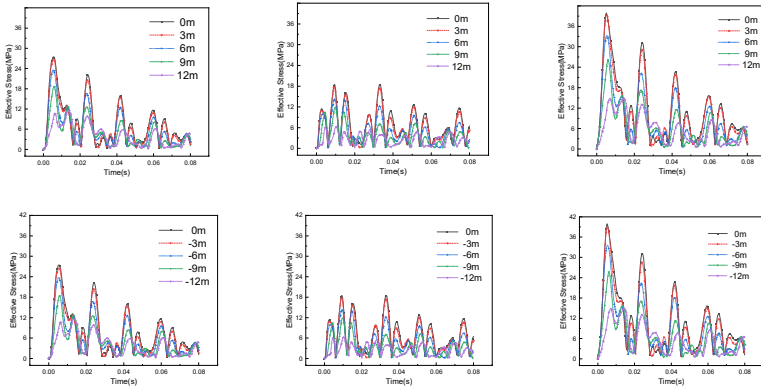


Fig. 9. The von-mises-stress time history curves of the sidewall, roof and corner positions in the upwind and downwind areas

Under closed conditions, Figure 8 and Figure 9 reveal that when the gas tank leaks and the gas block explodes under closed conditions, the selected stress distribution in the upper and lower wind direction areas affects the position of the corner area where the roof, side walls and gas tank bulkhead meet easily. The shock wave generated at the moment when the gas block explodes affects the stress concentration distribution on the gas bulkhead around the exploded gas block (Figure 8 a); after the shock wave encounters the gas tank bulkhead, it is reflected, and the shock waves in multiple directions will meet and superimpose, and the gas tank The corner area where the bulkheads meet limits the propagation path of the shock wave, making it difficult to disperse the energy evenly. The stress corresponds to a higher stress peak in the corner area (Figure 8 c)), and then a peak value appears on the side wall (Figure 8 d)), while the roof only The peak stress of the shock wave received from below is relatively small and delayed (Figure 8 e)). Then the shock wave propagates toward the cabin (Figure 8 b), 8 f)). During the process, due to the interaction between the shock wave and the internal structure of the pipe gallery, the energy gradually attenuates, and the stress amplitude gradually decreases and becomes stable.

Comparative Analysis of Three Working Conditions.

1) Displacement response.

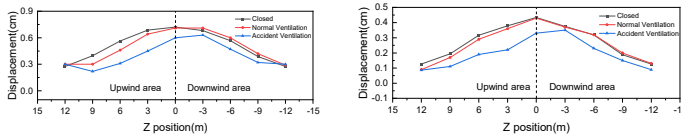


Fig. 10. Peak displacement curve of gas tank measuring point 1 and measuring point 2

It can be seen from Figure 10 that the peak displacement change curve of the structural measuring points 1 and 2 of the gas cabin in the event of a gas explosion under closed conditions is the largest. As the number of ventilations increases, the peak displacement curve of the measuring point gradually decreases, especially at the leakage hole. In the upwind area, the peak displacement change curve of the measuring point in the aggregation structure of the explosive gas block is significantly reduced due to the presence of fewer explosive gas blocks.

2) Stress distribution in the gas tank.

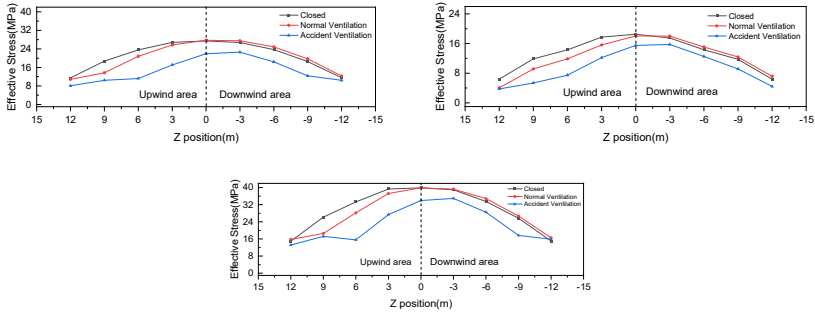


Fig. 11. Stress peak variation curves at the side walls, roof and corners of the gas tank

It can be seen from Figure 11 that the peak stress change curves of the structural side walls, roofs, and corners of the gas cabin in the event of a gas explosion under closed conditions are the largest. As the number of ventilations increases, the peak stress change curves of the measuring points gradually decrease, especially in In the upwind area of the leak hole, the peak stress variation curve of the measuring point at the measuring point is significantly reduced due to the presence of fewer explosive gas blocks.

4 Conclusion

(1) Under closed conditions, the displacement dynamic response of the measuring point is the largest when the gas tank explodes, indicating that the structural damage is the most severe under this condition. As the frequency of ventilation increases, the dynamic response gradually decreases, and the degree of structural damage also decreases accordingly. Therefore, in the design of comprehensive pipeline corridor projects, appropriately increasing the ventilation times can effectively reduce the risk of explosion accidents.

(2) The measuring points near the explosion point of the leak hole show the highest dynamic response and severe damage due to the direct impact of the shock wave. As the ventilation frequency increases, the explosive gas in the downwind area increases, making the measuring points in this area respond higher than those in the upwind area, and the damage is more serious. Therefore, in order to prevent gas explosion

accidents, it is recommended to install methane detectors downwind of potential leakage points such as gas pipeline valves, joints and welds in underground pipe galleries.

(3) The corner area where the gas tank bulkheads meet limits the propagation path of the shock wave, making it difficult to disperse the energy evenly, and the stress correspondingly appears to have a higher stress peak in the corner area. Therefore, chamfers should be set at the intersection of the walls at the corners of the gas tank to reduce stress concentration and enhance the explosion resistance of the structure.

References

1. Le Z, Tinghe Z, Weijun Z. (2021) Safety assessment of gas pipe gallery in most unfavorable leakage condition [J]. *Oil & Gas Storage and Transportation*,40(2): 200-207. 10.16265/j.cnki.issn1003-3033.2004.05.020.
2. Kun C, Hao L, Jie C, et al. (2023) Simulation study on leakage and diffusion of small holes in integrated pipe gallery gas pipelines under ventilation conditions [J]. *Journal of Safety and Environment*, 23: 3545-3553. 10.13637/j.issn.1009-6094.2022.1480.
3. Hua S, Cong T, Ning Z, et al. (2021) Effect of pipeline pressure on natural gas leakage and diffusion in natural gas pipe compartments of integrated pipeline corridors [J]. *Industrial safety and environmental protection*, 47(10): 31-34+74.
4. Xiling Q, Xiaoyan Y, Jiangping Z. (2017) Simulation study on leakage and diffusion of natural gas pipelines in underground comprehensive pipeline corridors [J]. *China's production safety science and technology*, 13(11): 85-89.
5. Xiaoqiao D, Anlin Y, Taolong X, et al. (2019) Research on the leakage and diffusion rules of gas transmission pipelines in gas cabins of urban comprehensive pipe corridors [J]. *China's production safety science and technology*, 15: 84-89.
6. KINDRACKI J, KOBIERA A, RARATA G, et al. (2007) Influence of ignition position and obstacles on explosion development in methane-air mixture in closed vessels[J]. *Journal of Loss Prevention in the Process Industries*, 20(4-6): 551-561. 10.1016/j.jlp.2007.05.010.
7. Zhipeng L, Shunchuan W, Qiong Y, et al. (2018) Research on numerical analysis of tunnel gas explosion and determination of explosion source type [J]. *Vibration and Shock*, 37: 94-101+140. 10.13465/j.cnki.jvs.2018.14.013.
8. SALZANO E, CAMMAROTA F, BENEDETTO A D. (2012) Explosion behavior of hydrogen-methane/air mixtures[J]. *Journal of Loss Prevention in the Process Industries*, 25(3): 443-447. 10.1016/j.jlp.2011.11.010.
9. Jicheng L, Chengbo L, Xueming Z, et al. (2017) Engineering technical standards for urban integrated pipe gallery monitoring and alarm systems [Z]. GB/T 51274-2017. Ministry of Housing and Urban-Rural Development of the People's Republic of China; General Administration of Quality Supervision, Inspection and Quarantine of the People's Republic of China.
10. Sanjiang L, Junqiang W, Renyang W, et al. (2017) Risk-based guidelines for grading safety hazards in oil and gas pipelines [Z]. GB/T 34346-2017. General Administration of Quality Supervision, Inspection and Quarantine of the People's Republic of China; National Standardization Administration of China.
11. Hengdong W, Weichen X, Xiangjing D, et al. (2015) Technical specifications for urban comprehensive pipe corridor engineering [Z]. GB 50838-2015. Ministry of Housing and Urban-Rural Development of the People's Republic of China; General Administration of Quality Supervision, Inspection and Quarantine of the People's Republic of China.

Open Access This chapter is licensed under the terms of the Creative Commons Attribution-NonCommercial 4.0 International License (<http://creativecommons.org/licenses/by-nc/4.0/>), which permits any noncommercial use, sharing, adaptation, distribution and reproduction in any medium or format, as long as you give appropriate credit to the original author(s) and the source, provide a link to the Creative Commons license and indicate if changes were made.

The images or other third party material in this chapter are included in the chapter's Creative Commons license, unless indicated otherwise in a credit line to the material. If material is not included in the chapter's Creative Commons license and your intended use is not permitted by statutory regulation or exceeds the permitted use, you will need to obtain permission directly from the copyright holder.

